JOURNAL OF SOLID STATE CHEMISTRY 111, 141–146 (1994)

Synthesis, Structure, and Physical Properties of $La_{3-x}M_xNi_2O_{7-\delta}$ ($M = Ca^{2+}$, Sr^{2+}, Ba^{2+}; $0 < x \leq 0.075$)

Z. Zhang and M. Greenblatt[1]

Department of Chemistry, Rutgers, The State University of New Jersey, Piscataway, New Jersey 08855

Received November 2, 1993; accepted January 13, 1994

IN HONOR OF C. N. R. RAO ON HIS 60TH BIRTHDAY

The synthesis, structure, and physical properties of $La_{3-x}M_xNi_2O_{7-\delta}$, with $M = Ca^{2+}$, Sr^{2+}, or Ba^{2+}, and $0 < x \leq 0.075$, were investigated. These compounds were prepared by a precursor method with tetramethyl ammonium hydroxide and were characterized by room temperature and high-temperature powder X-ray diffraction, TGA, electrical resistivity, and magnetic susceptibility measurements. The substituted compounds form with orthorhombic symmetry in space group *Fmmm*, similar to the as-prepared parent compound, $La_3Ni_2O_{6.92}$. As the amount of divalent alkaline earth metal substitution increases, the *c* cell parameter does not significantly change for Ca and increases significantly for Sr and Ba substitution, while the *a* and *b* cell parameters remain nearly unchanged for all cases. The observed trend in the *c* parameter is due to the increasing Ni^{3+} ion concentration for the case of Ca^{2+} substitution, while for Sr^{2+} and Ba^{2+} substitutions the effective larger size of the divalent cations is dominant. Significant oxygen deficiencies are noted in all of the as-prepared samples. However, upon high-pressure oxygen annealing, stoichiometric oxygen contents can be achieved. The room temperature resistivity of the as-prepared substituted compounds decreases relative to $La_3Ni_2O_{6.92}$, and at $x = 0.075$ a semiconductor to metal transition is observed for all *M*. The high-pressure oxygen annealed samples for all compositions show metallic behavior from room temperature down to 20 K. The magnetic susceptibility is nearly temperature independent in the temperature range 100–300 K, and paramagnetic behavior is observed below 100 K.

INTRODUCTION

The Ruddlesden–Popper phases (RP) (1) of lanthanum nickelates, with the general formula $(LAO)(LaNiO_3)_n$ or $La_{n+1}Ni_nO_{3n+1}$ ($n = 1, 2, 3 \cdots \infty$), are known to have two-dimensional (2D) structures and anisotropic electronic properties when *n* is a finite number (2). The structure is made up of *n* conducting perovskite-like layers ($LaNiO_3$) separated by insulating rock-salt-like layers (LaO) along the crystallographic *c* axis of the orthorhombic or tetragonal unit cell (Fig. 1). The NiO_6 octahedral corner share, extending infinitely in the *ab* plane, and *n* units of such planes stack in the *c* direction to form the perovskite slab. With increasing *n*, the width of the perovskite slab increases, with a concomitant increase of the electronic correlations along *c*. As a consequence, the electrical conductivity is enhanced from semiconductor (La_2NiO_4, $n = 1$) to metallic ($LaNiO_3$, $n = \infty$) with increasing *n*.

The structure and electronic properties of the RP nickelates are very similar to those of the high-temperature superconducting cuprates. Further, the recent discovery of diamagnetism in $La_2NiO_{4+\delta}$ and $La_{2-x}M_xNiO_4$ (M = Sr, Ca) (3) at low temperature renewed interest in the RP nickelates, partly for the possibility of finding superconductivity in these compounds.

Recently, we have investigated the structural and physical properties of the Ruddlesden–Popper nickelate, $La_3Ni_2O_{7-\delta}$ (4). This, and previous studies of the as-prepared sample with empirical formula $La_3Ni_2O_{6.92}$, revealed the presence of Anderson localization and semiconducting properties from room temperature down to 20 K (5). Reduction (in H_2/Ar) of the as-prepared sample further enhanced the electronic localization and decreased the conductivity of the sample. With high-pressure oxygen annealing of the as-prepared sample, a metallic, stoichiometric $La_3Ni_2O_{7.0}$ compound was obtained with Pauli-paramagnetic properties. The objective of this work was to investigate the effect of substitution of the divalent alkaline earth metals for La in $La_{3-x}M_xNi_2O_{7-\delta}$ (M = Ca, Sr, and Ba) on the structure/properties of RP nickelates.

EXPERIMENTAL

A detailed discussion of the synthetic procedure can be found in Ref. (4). A typical preparation involved stoichiometric amounts of La_2O_3 (99.99%, dried at 1000°C prior to use), MCO_3 (M = Ca, Sr, and Ba of 99.99% purity), and NiO (99.99%) dissolved in 3 *M* nitric acid solution to

[1] To whom correspondence should be addressed.

0022-4596/94 $6.00

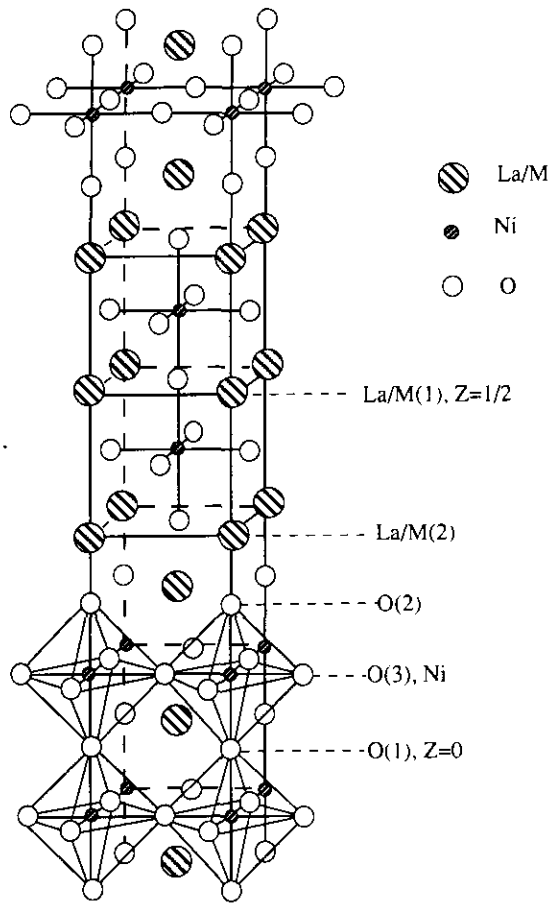

FIG. 1. The idealized structure of $La_{3-x}M_xNi_2O_{7-\delta}$.

which a 25% aqueous solution of tetramethyl ammonium hydroxide (TMA) was slowly added until a light-green precipitate was formed. The solution with the precipitate was gently heated to dryness on a hot plate. The resulting light-green solid was heated at 350°C in air to decompose the organic precursor, yielding a dark-gray powder. This powder was well ground and pressed into pellets. The pellets were calcined in air at 1130–1180°C in a high-density alumina crucible for 5–7 days. The heating temperature required for single-phase formation decreased slightly with increasing amounts of substitution; this shows that high-valent nickel compounds are favored at lower sintering temperature. Several intermittent grindings, followed by repelletization, were necessary to obtain single-phase $La_{3-x}M_xNi_2O_{7-\delta}$ (M = Ca^{2+}, Sr^{2+}, or Ba^{2+}, and $0 < x \leq 0.075$). Air quenching of the samples was required to avoid the formation of the low-temperature stable phase, $La_4Ni_3O_{10}$. To increase the crystallinity of the samples formed, the pellets were annealed in air at 500°C overnight, followed by furnace cooling. The high-pressure oxygen annealing was performed at 500°C under about 70 atm of oxygen for 24 hr in a Leco high-pressure apparatus.

Room temperature and high-temperature powder X-ray diffraction (PXD) data, collected on a SCINTAG PAD V X-ray diffractometer with monochromatized Cu$K\alpha$ radiation and with Mica (NBS-675) as an internal standard, were used in the least-squares refinement of the unit-cell parameters. The scan rate was 1° 2θ per min with chopper increments of 0.01° 2θ in the range $20° \leq 2\theta \leq 80°$.

The oxygen content was determined by thermogravimetric analysis with a DuPont 951 thermogravimetric analyzer in a reducing atmosphere (11% H_2 in Ar). The heating rate was 2°C/min and the gas flow rate was about 35 cc/min. The iodometric titration was used to confirm the TGA results.

The electrical resistivity of pressed pellets was measured with a standard four-probe technique with a closed-cycle cryostat (APD Cryogenics, DE202) in the temperature range 20–300 K. A SQUID magnetometer (MPMS, Quantum Design) was used to measure the magnetic susceptibility of samples in the temperature range 4–300 K at an applied magnetic field of 1000 G.

RESULTS AND DISCUSSION

a. Synthesis

Some difficulties were experienced in obtaining pure phases of both the parent and the substituted compounds. A conventional solid-state reaction resulted in a mixture of the La_2NiO_4, $La_3Ni_2O_7$, and/or alkaline earth metal oxides. It is well established that decomposition of precursors with small particle size and high surface area often permits the preparation of homogeneous pure phases inaccessible by conventional solid-state reactions (6, 7). We were successful in synthesizing the parent compound $La_3Ni_2O_{7-\delta}$ with a TMA precursor (4). However, the substitution of alkaline earth metals in $La_{3-x}M_xNi_2O_{7-\delta}$ makes the synthesis more difficult, and impurity, mainly La_2NiO_4, is evidenced by PXD. With up to seven intermittent regrindings and repelletizations; single-phasic $La_{3-x}M_xNi_2O_{7-\delta}$ (M = Ca, Sr, and Ba, $0 < x \leq 0.075$) without La_2NiO_4 can be obtained reproducibly (i.e., the sample is PXD pure, no more or less than ~5% of La_2NiO_4 is present). When $x > 0.075$, La_2NiO_4 is always present in the PXD of all substituted phases even with more than 10 intermittent grindings and prolonged heating.

b. Structure and Cell Parameters

Similar to the parent compound, the substituted RP phases $La_{3-x}M_xNi_2O_{7-\delta}$ also form with a face-centered orthorhombic symmetry in space group *Fmmm*. The cell

TABLE 1

The Cell Parameters, Oxygen Content, and Orthorhombic to Tetragonal Transition Temperature of As-Prepared $La_{3-x}M_xNi_2O_{7-\delta}$

Compounds	a (Å)	b (Å)	c (Å)	$T_c \pm 3$°C
$La_3Ni_2O_{6.92\pm0.03}$	5.396(1)	5.450(1)	20.522(4)	350
$La_{2.975}Ca_{0.025}Ni_2O_{6.92\pm0.03}$	5.401(1)	5.449(1)	20.519(6)	—
$La_{2.95}Ca_{0.05}Ni_2O_{6.92\pm0.03}$	5.401(1)	5.446(1)	20.515(6)	—
$La_{2.925}Ca_{0.075}Ni_2O_{6.92\pm0.03}$	5.400(1)	5.445(1)	20.503(5)	—
$La_{2.975}Sr_{0.025}Ni_2O_{6.92\pm0.03}$	5.405(1)	5.454(1)	20.530(8)	325
$La_{2.95}Sr_{0.05}Ni_2O_{6.92\pm0.03}$	5.402(1)	5.449(1)	20.540(5)	300
$La_{2.925}Sr_{0.075}Ni_2O_{6.92\pm0.03}$	5.402(1)	5.445(2)	20.558(7)	275
$La_{2.975}Ba_{0.025}Ni_2O_{6.92\pm0.03}$	5.408(2)	5.454(2)	20.534(8)	—
$La_{2.95}Ba_{0.05}Ni_2O_{6.92\pm0.03}$	5.406(1)	5.448(1)	20.568(5)	—
$La_{2.925}Ba_{0.075}Ni_2O_{6.92\pm0.03}$	5.416(1)	5.448(1)	20.596(6)	—

TABLE 2

The Unit Cell Parameters and Oxygen Content of Oxygenated $La_{3-x}M_xNi_2O_7$

Compounds	a (Å)	b (Å)	c (Å)
$La_3Ni_2O_{7.00\pm0.03}$	5.396(1)	5.449(1)	20.516(4)
$La_{2.975}Ca_{0.025}Ni_2O_{7.00\pm0.03}$	5.403(1)	5.451(1)	20.503(6)
$La_{2.95}Ca_{0.05}Ni_2O_{7.00\pm0.03}$	5.402(1)	5.448(1)	20.476(6)
$La_{2.925}Ca_{0.075}Ni_2O_{7.00\pm0.03}$	5.409(1)	5.450(1)	20.422(5)
$La_{2.975}Sr_{0.025}Ni_2O_{7.00\pm0.03}$	5.401(1)	5.454(1)	20.519(8)
$La_{2.95}Sr_{0.05}Ni_2O_{7.00\pm0.03}$	5.405(1)	5.449(1)	20.505(5)
$La_{2.925}Sr_{0.075}Ni_2O_{7.00\pm0.03}$	5.405(2)	5.451(2)	20.430(7)
$La_{2.975}Ba_{0.025}Ni_2O_{7.00\pm0.03}$	5.407(2)	5.455(2)	20.525(8)
$La_{2.95}Ba_{0.05}Ni_2O_{7.00\pm0.03}$	5.406(1)	5.451(1)	20.513(5)
$La_{2.925}Ba_{0.075}Ni_2O_{7.00\pm0.03}$	5.412(1)	5.452(1)	20.450(6)

parameters, presented in Table 1, were determined from least-squares refinement of the PXD data. With substitution, the a and b cell parameters remain nearly constant while the c parameter changes systematically according to the substituting elements (see Fig. 2).

The coordination number (CN) of La in $La_3Ni_2O_7$ is 9 (ionic radius, 1.36 Å) and 12 (ionic radius, 1.50 Å) (8). The ionic radius of Ca^{2+} is 1.32 Å in a 9- and 1.48 Å in a 12-coordination site. Thus, the effective ionic radius of La^{3+} is only about 0.02–0.04 Å larger than that of Ca^{2+} and one would expect little or no change in the c cell parameter upon Ca^{2+} substitution, consistent with the observed data in Table 1. The c cell parameter of both Sr^{2+}- and Ba^{2+}-substituted compounds increases significantly with increasing x, indicating the dominant effect of increasing ionic radius from La^{3+} to Sr^{2+}/Ba^{2+} ($r_{Sr^{2+}} = 1.45$ Å, $r_{Ba^{2+}} = 1.61$ Å for CN = 9; $r_{Sr^{2+}} = 1.58$ Å, $r_{Ba^{2+}} = 1.75$ Å for CN = 12) (8) over the effect of the increasing smaller Ni^{3+} ion content.

The unit cell parameters of the fully oxygenated $La_{3-x}M_xNi_2O_7$ phase in Table 2 show a systematic and significant decrease of the c parameter relative to the corresponding oxygen-deficient phase. This is attributed to the increase of Ni^{3+} content with increasing oxygen content; Ni^{3+} is smaller than Ni^{2+} as discussed earlier.

A structural phase transition from orthorhombic to tetragonal (O → T) symmetry has been observed in some of the RP nickelates (9). The O → T phase transition temperature, T_c, is a function of the phase distortion; i.e., the smaller the distortion of the orthorhombic phase from the tetragonal phase, the lower is T_c, which is affected by oxygen content and/or the nature and amount of the substituting species. To study the influence of alka-

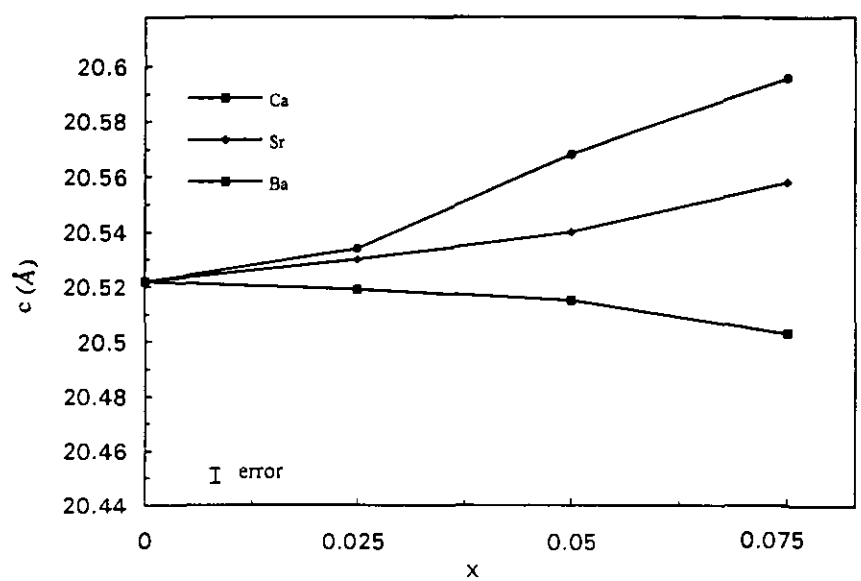

FIG. 2. Variation in the lattice parameter c as a function of substitution in as-prepared $La_{3-x}M_xNi_2O_{7-\delta}$, M = Ca, Sr, and Ba.

line earth metal substitution on the temperature of the O → T phase transition, high-temperature X-ray diffraction studies have been carried out to monitor the degree of the distortion for Sr-substituted samples; the transition temperatures (T_c) are listed in Table 1. The divergence of the X-ray diffraction peaks indexed as (2 0 0) and (0 2 0) were used as a relative measure of this distortion. With an increase of the temperature the splitting of these two peaks diminished and eventually disappeared at the critical temperature. The O → T phase transition temperature determined in this manner decreases with increasing x, which is paralleled by the change of the electrical resistivity discussed below.

c. Oxygen Content Analysis

The total oxygen content of all the samples was determined by TGA measurement with La_2O_3, Ni, and MO (M = Ca, Sr, Ba) as final products as evidenced by PXD. The iodometric titration was used to confirm the TGA results. The results are presented in Table 1, along with the unit cell parameters. The incorporation of small amounts of divalent cation into the oxygen-deficient parent compound does not change the oxygen content significantly. The oxygen nonstoichiometry present in both the parent and the substituted compounds is the same. Unlike in some of the K_2NiF_4-type compounds such as La_2NiO_4 and Nd_2NiO_4, extra oxygen is not required for the stabilization of the structure of doped or undoped $La_3Ni_2O_{7-\delta}$ where the relatively high Ni^{3+} content can stabilize the structure (9). The oxygen content can be increased to stoichiometric $La_{3-x}M_xNi_2O_{7.0}$ by high-pressure oxygen annealing.

d. Electrical Resistivity

The room temperature electrical resistivities and the temperature dependence of resistivities (ρ) for all samples have been measured. Because of the similar trend of the temperature dependence of the resistivity for all substitutions ($La_{3-x}M_xNi_2O_{7-\delta}$, M = Ca, Sr, and Ba), only the data of the Sr-substituted compounds are shown in Fig. 3. Metallic-like behavior is observed for the Sr-substituted samples with $0.05 \leq x \leq 0.075$ and for both Ca- and Ba-substituted samples with $x = 0.075$ in the temperature interval 120–200 K. All the other samples show semiconducting behavior. Substitution of a divalent cation for La has an effect on the electronic properties of $La_3Ni_2O_{7-\delta}$ similar to the introduction of oxygen in the structure (4). In both cases, the Anderson localization of

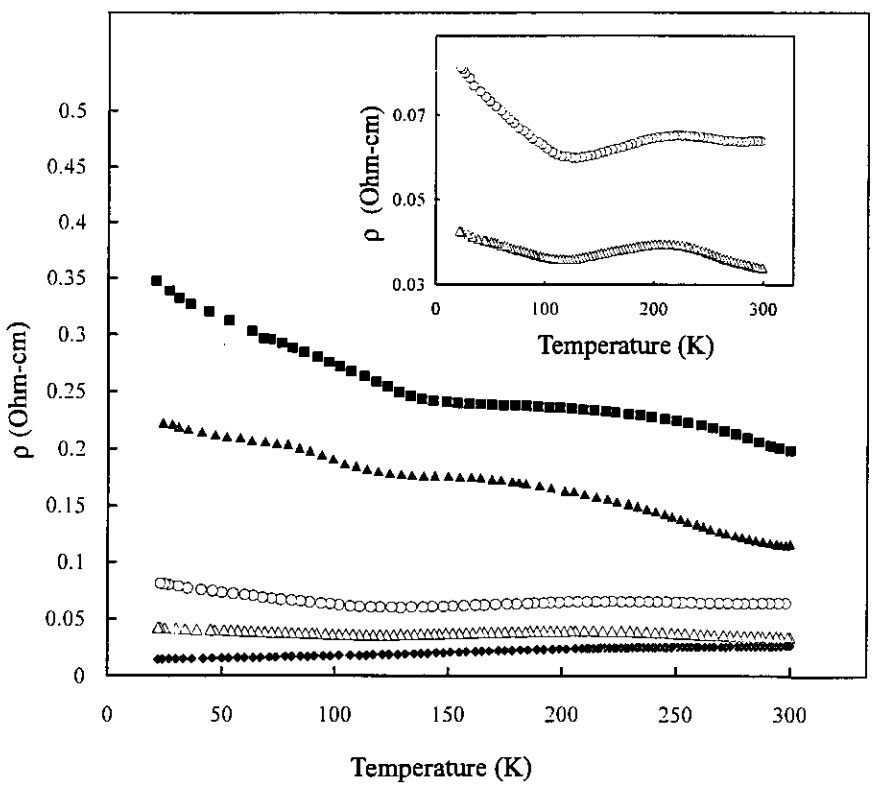

FIG. 3. Temperature dependence of resistivity for $La_{3-x}Sr_xNi_2O_{7-\delta}$, $0 \leq x \leq 0.075$. Solid square, $x = 0$; solid triangle, $x = 0.025$; open circle, $x = 0.05$; open triangle, $x = 0.075$ (all four are as-prepared samples); solid diamond, $x = 0.075$ (O_2 annealed sample). (Inset) Open circle, $x = 0.05$; open triangle, $x = 0.075$ (both are as-prepared samples).

states at the edge of the $\sigma^* x^2 - y^2$ band and in the middle of the correlation gap is significantly reduced. Furthermore, the enhancement of Ni^{3+} concentration leads to an increase in the number of charge carriers and stronger overlapping of the e_g orbitals of nickel and the p orbitals of oxygen. Thus, substitution of divalent cations for La^{3+} or oxygenation of $La_3Ni_2O_{7-\delta}$ will result in progressive delocalization of the e_g electrons and hence metallic behavior. The decrease of room temperature resistivity with increasing M^{2+} substitution, and consequent Ni^{3+} content, confirms the correlation between the electronic properties and the nickel formal valence. There are indications of localization, probably due to electrons trapped at oxygen defects, taking place at low temperature in the ρ vs T data (see inset of Fig. 3). The high-pressure oxygen annealing has increased the oxygen content to $La_{3-x}M_xNi_2O_7$. As in $La_3Ni_2O_7$, this leads to lower room temperature resistivity and stronger metallic behavior down to 20 K. These results provide further evidence for the qualitative accuracy of the band diagram we proposed earlier (4).

In contrast to $La_{2-x}Sr_xNiO_4$ (10, 11) and $Nd_{2-x}Sr_xNiO_4$ (9), where metallic behavior is only achieved with $x \approx 50\%$, $La_{3-x}M_xNi_2O_{7-\delta}$ becomes metallic with very small amounts (less than 4%) of alkaline earth ion substitution. These results are consistent with the effect of dimensionality on the physical properties.

It is noteworthy that the Sr-doped compounds have the lowest resistivity of $La_{3-x}M_xNi_2O_{7-\delta}$ (M = Ca, Sr, and Ba) phases. The dependence of the resistivity on the nature of the divalent cation can be attributed to the size effect on the tolerance factor (t) for the perovskite related structure. The t is defined as (2)

$$t = (r_{La-O})/\sqrt{2}r_{Ni-O}),$$

where r_{La-O} and r_{Ni-O} refer to the sum of covalent radii of the La–O (or M–O) and Ni–O bonds. The perovskite structure is stable over the range $0.85 < t < 1$. Since the value of $t \sim 0.91$, is close to the lower limit for $La_3Ni_2O_{7-\delta}$, the replacement of the trivalent cation with a larger divalent cation may be sufficient to stabilize the structure. Both Sr^{2+} and Ba^{2+} have larger ionic radii than that of La^{3+}; with complete substitution of Sr^{2+} and Ba^{2+} for La^{3+}, t increases to 0.95 and 1.01, respectively. Thus, partial Sr^{2+} substitution for La^{3+} leads to optimal stabilization of the structure and to the concomitant lowest electrical resistivity. This effect is similar to that seen in the high-T_c superconductors $La_{2-x}M_xCuO_4$ (M = Ca, Sr, Ba), where $La_{2-x}Sr_xCuO_4$ exhibits the highest superconducting transition temperature among all three alkali earth metal-substituted lanthanum cuprates (12).

e. Magnetic Properties

The temperature dependence of the magnetic susceptibilities (χ), in the range 4–300 K, for $La_{3-x}Sr_xNi_2O_{7-\delta}$, is shown in Fig. 4. This χ behavior is representative for all

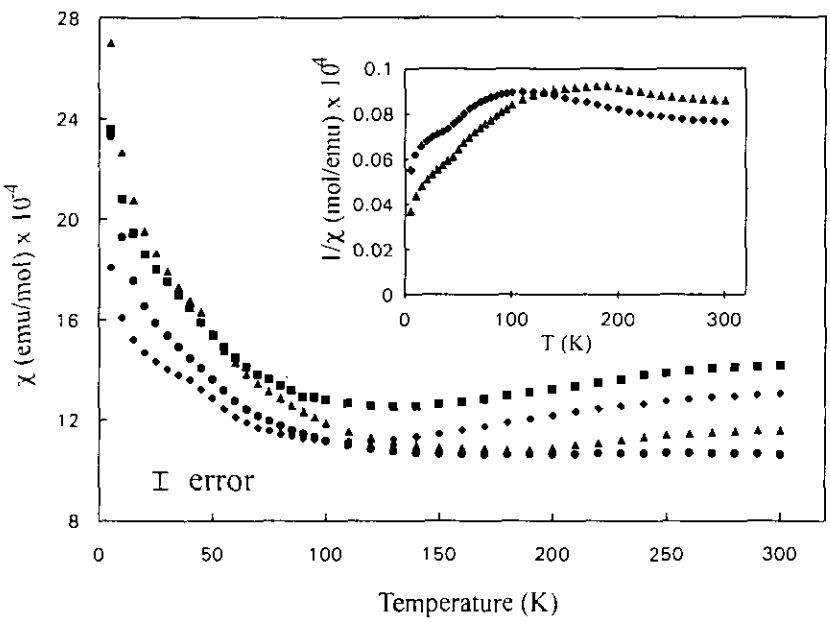

FIG. 4. Temperature dependence of susceptibility for representative samples of $La_{3-x}Sr_xNi_2O_{7-\delta}$. Diamond, $x = 0$; square, $x = 0.05$; triangle, $x = 0.075$ (all three are as-prepared samples). Circle, Sr = 0.075 (O_2 annealed sample). (Inset) Temperature dependence of $1/\chi$ for representative samples. Diamond, $x = 0$; triangle, $x = 0.075$ (both are as-prepared samples).

M^{2+} substitutions. In the high-temperature region ($T >$ 100 K), the susceptibilities of all the samples remain nearly temperature independent, indicative of delocalized or partially delocalized electrons, and are consistent with the low resistivity semiconducting or metallic behavior in that temperature region. The differences seen in the room temperature χ values in Fig. 4 are significant within the experimental error; however, the changes observed are not systematic and are therefore currently unclear. The χ of the as-prepared substituted samples decreases slightly with decreasing temperature in the temperature range 120–300 K. This observation of decreasing χ with decreasing temperature in the high-temperature region can be attributed to short-range Ni^{2+}–O–Ni^{2+} antiferromagnetic interactions. With increasing Ni^{3+} content the Ni^{3+}–O–Ni^{2+} ferromagnetic interactions are enhanced so the rate of decrease of χ as a function of temperature diminishes for the M^{2+}-substituted and/or high-pressure oxygenated phases.

The variation of the inverse susceptibility with temperature does not follow the Curie–Weiss behavior for all the samples (Fig. 4, inset). The deviation from the Curie–Weiss law may well reflect the existence of short-range ferromagnetic and/or antiferromagnetic correlations.

Below 100 K, the paramagnetic behavior, consistent with the upturn in the ρ vs T data, probably due to localized electrons at oxygen defects, dominates the susceptibilities of all the samples (Fig. 4).

CONCLUSIONS

A new solid-solution series of $La_{3-x}M_xNi_2O_{7-\delta}$ (M = Ca, Sr, and Ba, and $0 < x \leq 0.075$) have been successfully synthesized by a precursor method. The X-ray powder diffraction patterns can be indexed based on an orthorhombic unit cell with space group *Fmmm*. The unit cell parameter c displayed systematic variations as a function of the amount of substitution and size of the divalent cation. The c cell parameter in the case of Ca^{2+} substitution is unchanged. With increasing Sr^{2+} or Ba^{2+} content, the c parameter increases due to the dominant effect of substitution by the larger $M = Sr^{2+}$, Ba^{2+} cations for La^{3+}. The temperature-dependent resistivity measurements indicated semiconducting behavior for $0 < x \leq 0.05$, a gradual decrease of the room temperature resistivity with progressive increase of x, and a semiconductor to metal transition for $x = 0.075$ for all M. The magnetic susceptibility measurements show a nearly temperature-independent behavior over the temperature region $100 < T < 300$ K, consistent with partially delocalized electrons. The deviation of $1/\chi$ vs T from ideal Curie–Weiss behavior above 100 K has been ascribed to short-range antiferromagnetic and/or ferromagnetic interactions of the type Ni^{2+}–O–Ni^{2+} and/or Ni^{3+}–O–Ni^{2+}, respectively.

ACKNOWLEDGMENTS

The authors thank Dr. K. V. Ramanujachary for helpful discussions. This work was supported by National Science Foundation Solid State Chemistry Grant DMR-90-19301.

REFERENCES

1. S. N. Ruddlesden and P. Popper, *Acta Crystallogr.* **11,** 541 (1958).
2. J. B. Goodenough and J. M. Longo, "Landolt-Börnstein, New Series III," Vol. 4a, p. 193. Springer-Verlag, New York/Berlin, 1970.
3. K. S. Nanjundaswamy, A. Lewicki, Z. Kakol, P. Gopalan, P. Metcalf, J. M. Honig, C. N. R. Rao, and J. Spalek, *Physica C* **166,** 361 (1990).
4. Z. Zhang, M. Greenblatt, and J. B. Goodenough, *J. Solid State Chem.* **108,** 402 (1994).
5. R. A. Mohan Ram, L. Ganapathi, P. Ganguly, and C. N. R. Rao, *J. Solid State Chem.* **63,** 139 (1986).
6. L. Wachowski, S. Zielinski, and A. Burewicz, *Acta Chim. Acad. Sci. Hung.* **106,** 217 (1981).
7. S. Sundar Manoharan and K. C. Patil, *J. Solid State Chem.* **102,** 267 (1993).
8. R. D. Shannon, *Acta Crystallogr. A* **32,** 751 (1976).
9. B. W. Arbuckle, K. V. Ramanujachary, Z. Zhang, and M. Greenblatt, *J. Solid State Chem.* **88,** 278 (1990).
10. K. Sreedhar and C. N. R. Rao, *Mater. Res. Bull.* **25,** 1235 (1990).
11. Y. Takeda, R. Kanno, M. Sakano, O. Yamamoto, M. Takano, Y. Bando, H. Akinaga, K. Takita, and J. B. Goodenough, *Mater. Res. Bull.* **25,** 293 (1990).
12. K. Oh-Ishi and Y. Syono, *J. Solid State Chem.* **95,** 136 (1991).